



**HAL**  
open science

## New semi-automatic method for reaction product charge and mass identification in heavy-ion collisions at Fermi energies

D. Gruyer, Eric Bonnet, A. Chbihi, J.D. Frankland, S. Barlini, B. Borderie, R. Bougault, J. A. Duenas, E. Galichet, A. Kordyasz, et al.

### ► To cite this version:

D. Gruyer, Eric Bonnet, A. Chbihi, J.D. Frankland, S. Barlini, et al.. New semi-automatic method for reaction product charge and mass identification in heavy-ion collisions at Fermi energies. 2016. in2p3-01348951v3

**HAL Id: in2p3-01348951**

**<https://hal.in2p3.fr/in2p3-01348951v3>**

Preprint submitted on 1 Dec 2016 (v3), last revised 13 Dec 2016 (v4)

**HAL** is a multi-disciplinary open access archive for the deposit and dissemination of scientific research documents, whether they are published or not. The documents may come from teaching and research institutions in France or abroad, or from public or private research centers.

L'archive ouverte pluridisciplinaire **HAL**, est destinée au dépôt et à la diffusion de documents scientifiques de niveau recherche, publiés ou non, émanant des établissements d'enseignement et de recherche français ou étrangers, des laboratoires publics ou privés.

# New semi-automatic method for reaction product charge and mass identification in heavy-ion collisions at Fermi energies

D. Gruyer<sup>a,b,\*</sup> E. Bonnet<sup>b</sup> A. Chbihi<sup>b</sup> J.D. Frankland<sup>b</sup>  
S. Barlini<sup>a,c</sup> B. Borderie<sup>d</sup> R. Bougault<sup>e</sup> J. A. Dueñas<sup>f</sup>  
E. Galichet<sup>d,g</sup> A. Kordyasz<sup>h</sup> T. Kozik<sup>i</sup> N. Le Neindre<sup>e</sup>  
O. Lopez<sup>e</sup> M. Pârlog<sup>e,j</sup> G. Pastore<sup>a,c</sup> S. Piantelli<sup>a</sup> S. Valdré<sup>a,c</sup>  
G. Verde<sup>d,k</sup> E. Vient<sup>e</sup>

<sup>a</sup>*INFN – Sezione di Firenze, via Sansone 1, I-50019 Sesto Fiorentino, Italy*

<sup>b</sup>*Grand Accélérateur National d'Ions Lourds (GANIL), CEA/DRF–CNRS/IN2P3,  
Bvd. Henri Becquerel, 14076 Caen, France*

<sup>c</sup>*Dipartimento di Fisica, Università di Firenze, I-50019 Sesto Fiorentino, Italy*

<sup>d</sup>*Institut de Physique Nucléaire, CNRS/IN2P3, Univ. Paris-Sud, Université  
Paris-Saclay, Orsay, France*

<sup>e</sup>*Normandie Univ, ENSICAEN, UNICAEN, CNRS/IN2P3, LPC Caen, 14000  
Caen, France*

<sup>f</sup>*Departamento de Ingeniería Eléctrica, Escuela Técnica Superior de Ingeniería,  
Universidad de Huelva, 21819 Huelva, Spain*

<sup>g</sup>*Conservatoire National des Arts et Métiers, F-75141 Paris Cedex 03, France*

<sup>h</sup>*Heavy Ion Laboratory, University of Warsaw, ul. Pasteura 5A, 02-093 Warsaw,  
Poland.*

<sup>i</sup>*Faculty of Physics, Astronomy and Applied Computer Science, Jagiellonian  
University, 30-348 Cracow, Poland*

<sup>j</sup>*National Institute for Physics and Nuclear Engineering, RO-76900  
Bucharest-Màgurele, Romania*

<sup>k</sup>*INFN – Sezione di Catania, 64 Via Santa Sofia, I-95123 Catania, Italy*

---

## Abstract

This article presents a new semi-automatic method for charge and mass identification of charged nuclear fragments using either  $\Delta E - E$  correlations between measured energy losses in two successive detectors or correlations between charge signal amplitude and rise time in a single silicon detector, derived from digital pulse shape analysis techniques. In both cases different nuclear species (defined by their atomic number  $Z$  and mass number  $A$ ) can be visually identified from such correla-

tions if they are presented as a two-dimensional histogram ('identification matrix'), in which case correlations for different species populate different ridge lines ('identification lines') in the matrix. The proposed algorithm is based on the identification matrix's properties and uses as little information as possible on the global form of the identification lines, making it applicable to a large variety of matrices. Particular attention has been paid to the implementation in a suitable graphical environment, so that only two mouse-clicks are required from the user to calculate all initialization parameters. Example applications to recent data from both INDRA and FAZIA telescopes are presented.

*Key words:* Silicon Detector, Computer Data Analysis, Charged Particle Identification

---

## 1 Introduction

In the intermediate energy regime, violent heavy-ion collisions produce many nuclear species with a large range of charge ( $Z$ ), mass ( $A$ ), and kinetic energy ( $E_k$ ) [1,2]. Studying this kind of reactions requires detectors with almost  $4\pi$  solid angle coverage, high granularity, low energy thresholds, large dynamic range in energy and capable of characterizing reaction products on an event by event basis. The first generation of  $4\pi$  multi-detectors focused on complete collection of charged particles produced in a reaction [3,4,5,6,7], providing little isotopic information for heavy fragments ( $Z > 5$ ). More recently detectors have evolved to provide isotopic resolution for a broader range of products [8,9,10], by improving existing detectors and identification techniques, or developing new methods such as the Pulse Shape Analysis (PSA) in silicon detectors [11,12,13].

Such multi-detectors are generally made of telescopes (stacks of detector material layers) measuring the energy lost by charged particles in the different stages. Several combinations of detectors have been used for this purpose, such as ionization chambers (IC), silicon detectors (Si), plastic scintillators, and thallium-activated cesium-iodide scintillators (CsI(Tl)). When a charged particle passes through such a telescope, its charge, mass, and kinetic energy determine the number of detectors it can cross before stopping, and the energy loss in the different layers. Charged particles are then identified by plotting the energy loss in one or several layers of the telescope ( $\Delta E$ ) versus the residual energy released in the detector in which the particle is stopped ( $E$ ). Within

---

\* Corresponding author.

*Email address:* diego.gruyer@fi.infn.it (D. Gruyer).

24 this representation, called  $\Delta E - E$  matrix, different particles populate iden-  
25 tification lines characteristic of their charge and mass (see for example Fig.  
26 1(a)).

27 Three main methods are then used to identify such particles:

- 28 (i) Interactive drawing of lines in order to discriminate between the ridges  
29 corresponding to a given charge and/or mass. Particles are then identified  
30 from their relative distance between pairs of ridge lines.
- 31 (ii) Fit of a limited set of ridge lines with a functional describing the relation  
32 between  $\Delta E$  and  $E$ , in which  $Z$  and  $A$  enter as parameters [14,15,16,17].  
33 In this case, particle identification is obtained by inversion of the func-  
34 tional for given  $\Delta E$  and  $E$ , in order to extract  $Z$  and possibly  $A$ .
- 35 (iii) Fit of detector calibration parameters on a limited set of ridge lines  
36 using energy loss table to generate all identification lines [20,27,10,21].  
37 Particles are then identified from their relative distance between pairs of  
38 ridge lines.

39 The method (i) is probably more powerful and allows to face any situation,  
40 such as complex detector responses, but it suffers from two main limitations:  
41 it does not provide any extrapolation in regions of low statistics, and it is time  
42 consuming because each line has to be accurately drawn.

43 Methods (ii) and (iii) allow extrapolation and suffer less from this latter incon-  
44 venience, since only a subset of ridge lines have to be drawn by hand. It may  
45 still become problematic when using multidetectors composed of thousands  
46 of identification telescopes. In both cases, identification performances rely on  
47 the precise knowledge of the detector response, which can be very complex  
48 in the case of CsI(Tl) scintillators light output-energy conversion [18] or in  
49 presence of pulse-height defect in silicon detectors [19]. These two methods  
50 are very efficient in reproducing  $Z$  lines but are generally not accurate enough  
51 to reproduce isotopic lines over a large range of elements.

52 With increasing numbers of identification matrices to treat which include in-  
53 formation on increasing numbers of individual isotopes of different elements, it  
54 becomes essential to develop automatic or semi-automatic methods to extract  
55 identification lines in  $\Delta E - E$  matrices. The need for automation was already  
56 evident with the advent of the first large charged particle arrays, and some  
57 methods were developed at that time, using for example image processing  
58 [22,25,26], or artificial neural networks [23]. More recently, neural networks  
59 have been applied directly to digital current signal [13] for isotopic identi-  
60 fication. Cluster algorithms have also been used for proton- $\gamma$  discrimination  
61 [24].

62 The evolution of computer resources, and the availability of powerful libraries  
63 dedicated to large scale data analysis [28,29] allow us to consider new types of

64 algorithms. In this article we present a new method, called SPIDER<sup>1</sup> identi-  
65 cation (for Spider Particle Identification in  $\Delta E - E$  Representation) for semi-  
66 automatic ridge line determination in two-dimensional matrices. This method  
67 has been developed avoiding as much as possible the use of *a priori* informa-  
68 tion on the exact form of identification lines, in order to be applicable to a  
69 large variety of identification matrices. Particular attention has been payed to  
70 the implementation in a suitable graphical environment. The extracted lines  
71 can then be directly used to identify charged particles (i), or set as an input  
72 of a functional fit (ii) or energy loss fit (iii).

## 73 2 SPIDER identification

### 74 2.1 Algorithm

75 Determining ridge lines in two-dimensional matrices  $(x, y)$  is a hard task,  
76 whereas powerful algorithms for peak localization in  $N$ -dimensional matrices  
77 are available [30]. The main idea of the present method is then to transform our  
78 problem into a problem of peak localization in one-dimensional histograms.  
79 To do so, we have to project a part of the matrix onto a relevant axis. It is the  
80 shape of the identification lines and their relative population that guided the  
81 choice of this projection. The one-dimensional histogram shown in Fig. 1(b)  
82 is obtained by projecting all points between  $D(\theta - \alpha/2)$  and  $D(\theta + \alpha/2)$  onto  
83 the straight line  $D(\theta)$ , passing through  $(x_0, y_0)$  and making an angle  $\theta$  with  
84 respect to  $Ox$  (see Fig. 1(a) where  $x$  stands for  $E$  and  $y$  for  $\Delta E$ ). Each peak  
85 appearing on this projection corresponds to the intersection between  $D(\theta)$  and  
86 a ridge line of a given  $Z$  and  $A$ <sup>2</sup>. The angle of the first projection,  $\theta_0$ , and the  
87 pedestal coordinates  $(x_0, y_0)$  are input parameters of the algorithm.

To localize the peaks in Fig. 1(b), the binning of the histogram should be  
chosen carefully. The number of bins  $n_b$  of the projection is defined as:

$$n_b = d_\theta \times \rho(\theta) \times \beta, \quad (1)$$

with  $d_\theta$  the length of the projection,  $\beta$  a binning parameter to be provided by

<sup>1</sup> not to be confused with the ‘‘SpiderWeb’’ surface construction algorithm

<sup>2</sup> The ridge lines of individual isotopes are indistinguishable in these data, due to insufficient resolution of the  $\Delta E$  detectors. In this case ions of different  $Z$  populate broad ridges around the mean value  $\langle A \rangle$  of their isotopic distribution.

the user, and  $\rho(\theta)$  an internal parameter given by:

$$\rho(\theta) = \begin{cases} \sqrt{2} & \text{if } \theta > \theta_0 \\ 1 & \text{if } \theta = \theta_0 \\ 5/4 & \text{if } \theta < \theta_0. \end{cases} \quad (2)$$

88 The choice of  $\rho(\theta)$  is purely phenomenological.

89 Maxima are then located using the algorithm described in [30], and their  
 90 position in the two-dimensional matrix (Fig. 1(c)) is used as starting point for  
 91 all subsequently generated identification lines, making crucial the choice of  $\theta_0$ .

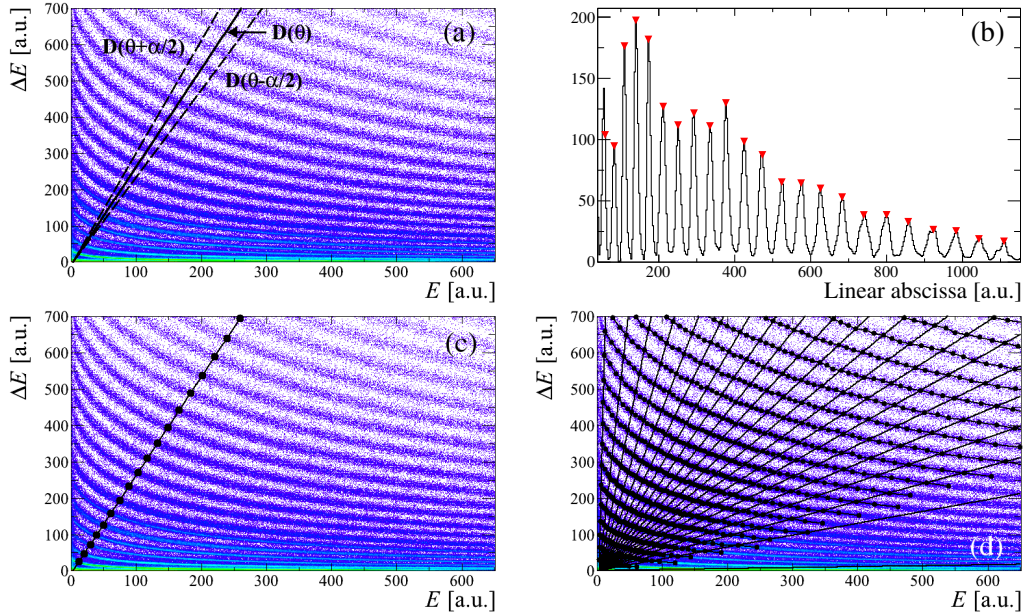


Fig. 1. Illustration of the different steps of the SPIDER identification: (a) definition of the projection; (b) projection on line  $D(\theta)$  and localization of maxima; (c) positioning of the maxima on the  $\Delta E - E$  matrix; (d) weaving of the spiderweb.

The operation of projection/localization is then repeated in order to cover the full matrix, varying  $\theta$  from  $\theta_0$  to  $90^\circ$ , and then from  $\theta_0$  to  $0^\circ$  by steps of  $\delta\theta$ . In practice,  $\delta\theta$  and  $\alpha$  slightly depend on  $\theta$ , and can be modified by the user in order to adapt the algorithm to a specific situation (very low statistics for example). Each new point  $P(x_p, y_p)$  is associated to the line  $Z$ , so far containing  $n_Z$  points and whose end point coordinates are  $(x_Z, y_Z)$ , if:

$$\begin{cases} |y_p - y_Z| < \delta y, & \text{for } n_Z < 10, \\ |y_p - f_Z(x_p)| < \delta y, & \text{for } n_Z \geq 10, \end{cases} \quad (3)$$

92 with  $f_Z(x) = a_Z^0 \times (x + a_Z^1)^{-a_Z^2}$  a function fitted to the  $n_Z$  points already  
 93 associated to the line  $Z$ , and  $\delta y = y_Z \times Z^{-1}$ . The choices of  $f_Z(x)$  and  $\delta y$  are

94 purely phenomenological.

Once the spiderweb is woven (see Fig. 1(d)), identification lines that do not fulfill the following criteria:

$$\begin{cases} n_Z > 10 \\ a_Z^1 < 3000 \\ 0.35 < a_Z^2 < 1 \end{cases} \quad (4)$$

95 are rejected, where  $n_Z$  is the final number of points associated to the line  
 96  $Z$ , and  $(a_Z^0, a_Z^1, a_Z^2)$  are the parameters of  $f_Z(x)$ . This procedure aims at  
 97 eliminating lines with a form completely incoherent with the Bethe-Bloch  
 98 formula, without being too restrictive in order for this method to be applicable  
 99 to different types of identification matrices.

100 It is then possible to build the identification grid from each of the individ-  
 101 ual functions  $f_Z(x)$ , either limited to the range where peaks were found (see  
 102 Fig.2 for example), or extrapolated over the whole residual energy range (see  
 103 Fig.4(a) for example).

## 104 2.2 Implementation

105 In order to run the algorithm presented above, several input parameters should  
 106 be provided by the user: the pedestal coordinates  $(x_0, y_0)$ , the first projection  
 107 angle  $\theta_0$ , and the binning parameter  $\beta$ . These parameters are generally difficult  
 108 to estimate, which makes our method unusable without an implementation  
 109 in a suitable graphical environment. It has therefore been included in the  
 110 identification grid editor of KaliVeda [29], which is a graphical user interface  
 111 dedicated to the creation and editing of identification grids developed initially  
 112 within the INDRA Collaboration [4].

The pedestal coordinates  $(x_0, y_0)$  can be set by the user with a simple click on  
 the  $\Delta E - E$  matrix. Our algorithm needs also another point,  $(X_0, Y_0)$ , situated  
 approximately in the middle of a high- $Z$  line; and the knowledge of the charge  
 $Z_0$  associated to this line. The values of  $\theta_0$  and  $\beta$  are then calculated as follows  
 :

$$\tan(\theta_0) = \frac{Y_0 - y_0}{X_0 - x_0} \quad (5)$$

$$\beta = \frac{1}{20Z_0} \sqrt{(X_0 - x_0)^2 + (Y_0 - y_0)^2}. \quad (6)$$

113 Thanks to the implementation in a “user friendly” graphical environment, our  
 114 method needs only two mouse-clicks from the user to calculate all initialization

115 parameters, making it very easy to use.

### 116 2.3 Examples of use

117 The present method has been initially developed to treat INDRA Si-CsI(Tl)  
118 matrices [4]. Since it uses as little information as possible on the exact form  
119 of  $Z$  lines, it can be applied to different types of identification telescopes.  
120 Here are several examples of use on Si-CsI(Tl), IC-Si, Si-Si matrices; and also  
121 matrices from Pulse Shape Analysis of the charge signal in silicon detectors.

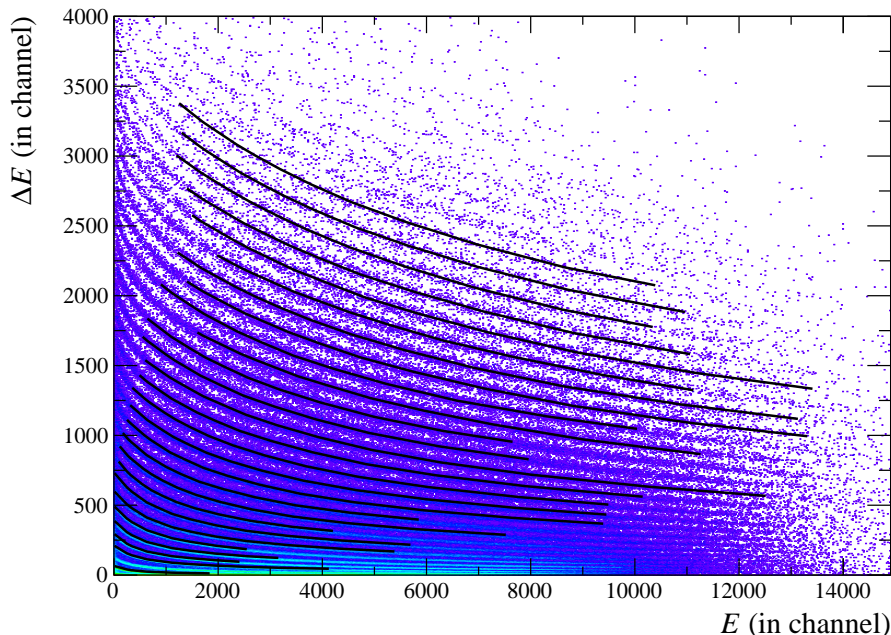


Fig. 2. Application of the SPIDER identification method on a Si-CsI(Tl) matrix of INDRA ( $\theta \sim 17^\circ$ ). Data come from the Ta+Zn at 39 MeV/A reaction measured at GANIL.

122 Fig. 2 presents the result of the SPIDER identification on a  $\Delta E - E$  matrix  
123 coming from a Si-CsI(Tl) telescope of the INDRA multidetector. In this ex-  
124 ample,  $Z$  lines up to  $Z = 29$  were found by our algorithm. Since extrapolation  
125 using individual functions is not safe in the case of Si-CsI(Tl) matrix, because  
126 of the strong curvature of  $Z$  lines at low residual energy ( $E$ ), identification  
127 lines have been generated on the range where points were found by the al-  
128 gorithm. The obtained identification grid cannot be used directly. It has to  
129 be completed by hand, or can be used as input to constrain a fit using some  
130 functional. This point is discussed in Section 2.4.

131 Fig. 3 presents the results of the SPIDER identification on a  $\Delta E - E$  matrix  
132 coming from an INDRA IC-Si telescope. In this kind of matrix,  $Z$  lines are

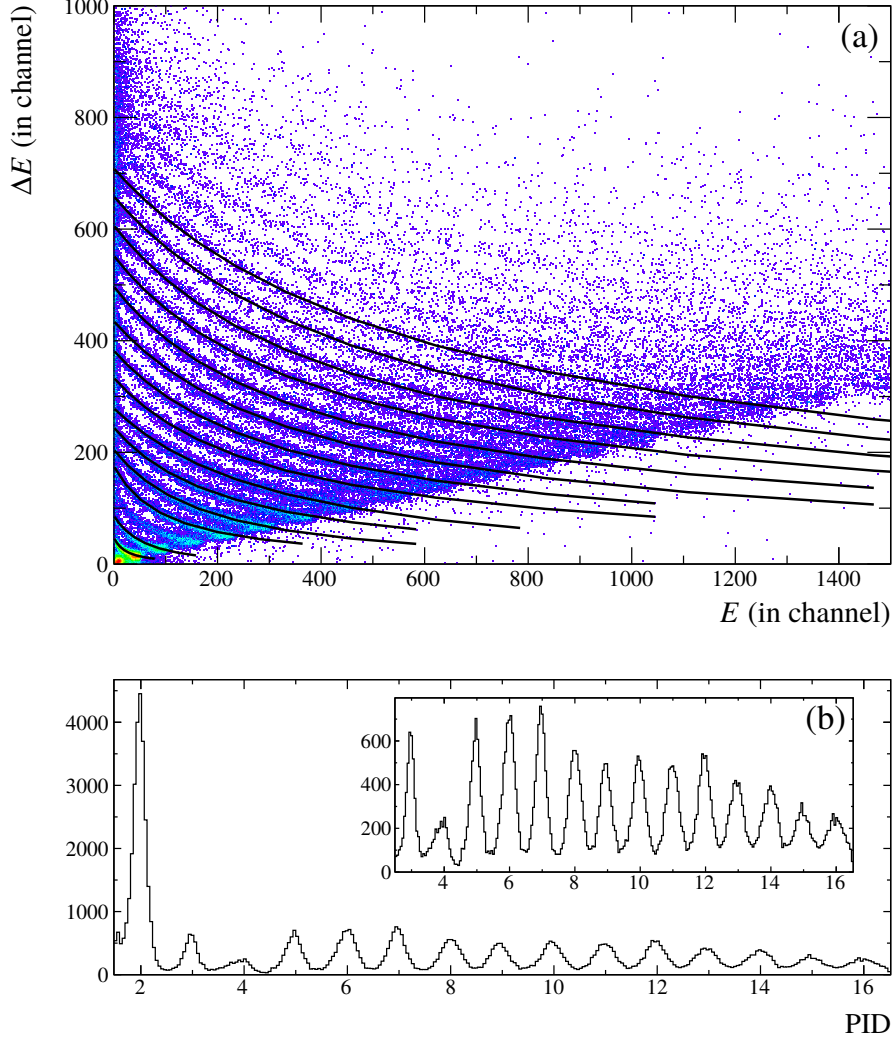


Fig. 3. Application of the SPIDER identification method on a IC-Si matrix of INDRA ( $\theta \sim 17^\circ$ ). PID stands for particle identification obtained after linearization of the matrix with the identification grid. Data come from the Ta+Zn at 39 MeV/A reaction measured at GANIL.

133 generally broad due to the poorer energy resolution of such large-area ioniza-  
 134 tion chambers operated at low pressure, and rarely homogeneously populated.  
 135 Nevertheless, our algorithm has extracted ridge lines from  $Z = 2$  to  $Z = 16$   
 136 (Fig. 3(a)), providing a good charge identification (Fig. 3(b)). It can be noted  
 137 that, in this example, the  $Z = 4$  line was not generated because it did not  
 138 satisfy the criteria of Eq. (4).

139 The result of the SPIDER identification on a  $\Delta E - E$  matrix coming from a  
 140 Si-Si telescope of FAZIA [9] is presented in Fig. 4. In this kind of matrix, ridge  
 141 lines corresponding to different elements are clearly separated thanks to the  
 142 very good quality of FAZIA silicon detectors. In addition, the line curvature is  
 143 quite slight, making the SPIDER identification very efficient (Fig. 4(a)). Even

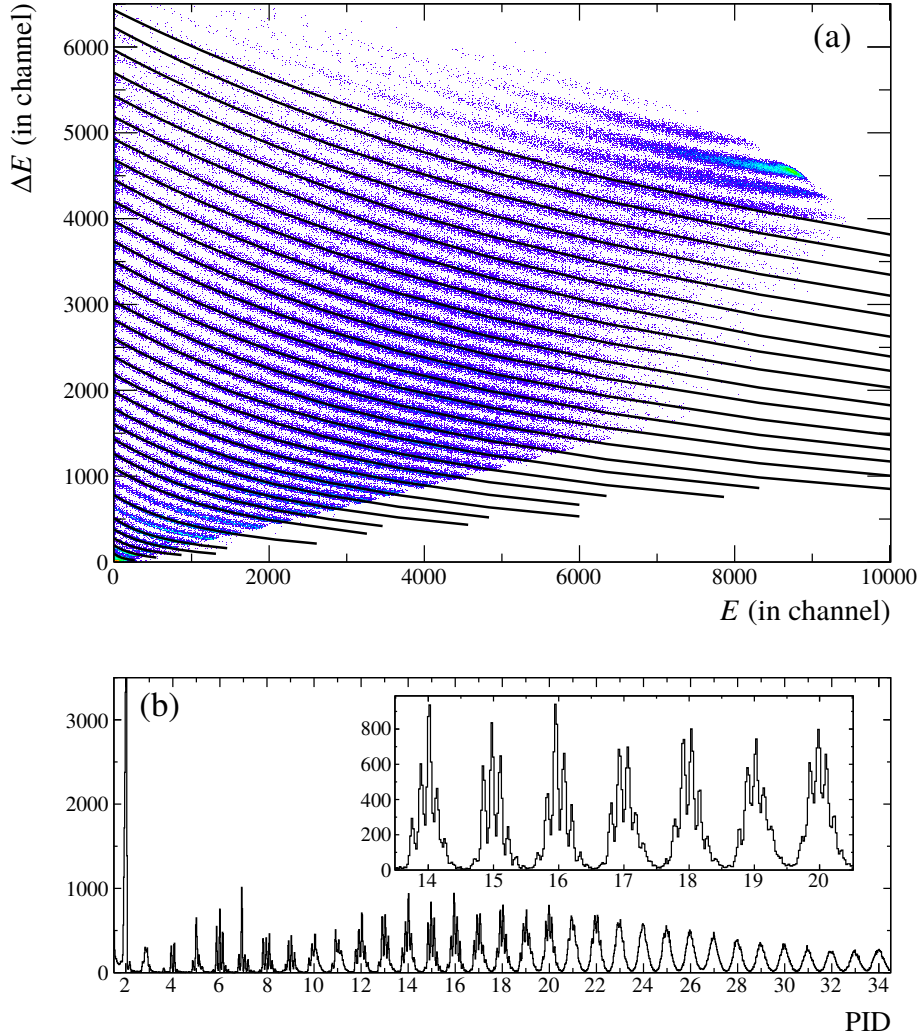


Fig. 4. Same as Fig. 3 for Si-Si matrix of FAZIA ( $\theta \sim 7^\circ$ ). Data come from the Kr+Sn at 35 MeV/A reaction measured at LNS [31,32].

144 if a few lines ( $Z = 7$  and  $Z = 9$ ) have not been generated, the grid provides  
 145 a very good charge identification, up to  $Z = 34$  (Fig. 4(b)). For each integer  
 146 value of  $Z$ , several peaks appear on the identification spectrum up to  $Z \sim 20$ .  
 147 These peaks correspond to different isotopes of each element, and allow to  
 148 discriminate particles of different masses. The charge-identification grid can  
 149 then be used as a starting point to generate a mass-identification grid. This  
 150 point is discussed in sec. 3.

151 Previous examples all concern the  $\Delta E - E$  method. Identification matrices  
 152 obtained by Pulse Shape Analysis of the charge signal in FAZIA silicon de-  
 153 tectors [9] present a form quite similar to that obtained with the  $\Delta E - E$   
 154 method. Since the SPIDER identification method uses little *a priori* informa-  
 155 tion on the ridge line form, it can also be applied to this type of matrix. In  
 156 the example shown in Fig. 5, the generated grid provides a satisfying charge

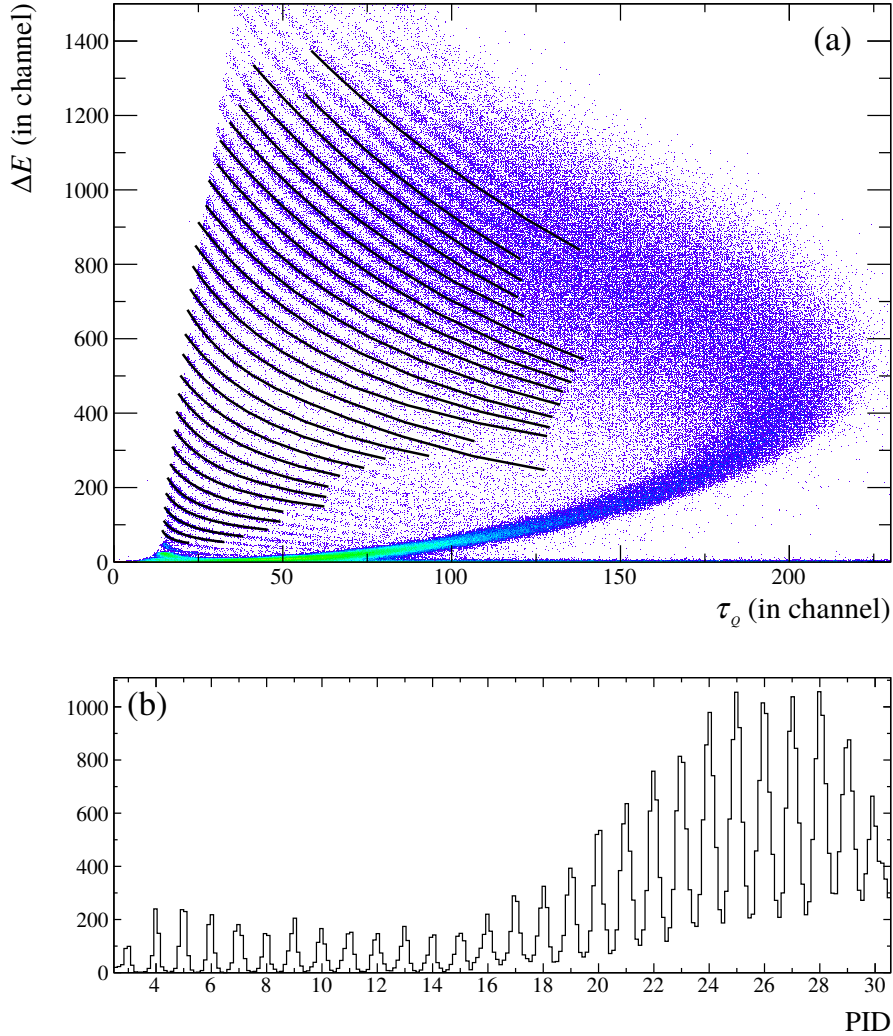


Fig. 5. Same as Fig. 3 for energy versus rise time of the charge signal in the first silicon layer matrix of FAZIA ( $\theta \sim 7^\circ$ ). Data come from the Kr+Sn at 35 MeV/A reaction measured at LNS [31,32].

157 identification from  $Z = 3$  up to  $Z = 30$  (Fig. 5(b)), even if identification lines  
 158 do not cover the full matrix range (Fig. 5(a)).

#### 159 2.4 Coupling with a fitting procedure

160 We have shown in previous examples that  $Z$ -lines generated by the SPIDER  
 161 identification, possibly extrapolated using individual functions, can be directly  
 162 used to identify particles. This procedure is efficient but does not allow to  
 163 extrapolate the identification to higher  $Z$ . These lines, without extrapolation,  
 164 can also be used as input to fit functional parameters. In the present example,  
 165 we used the functional proposed in [16].

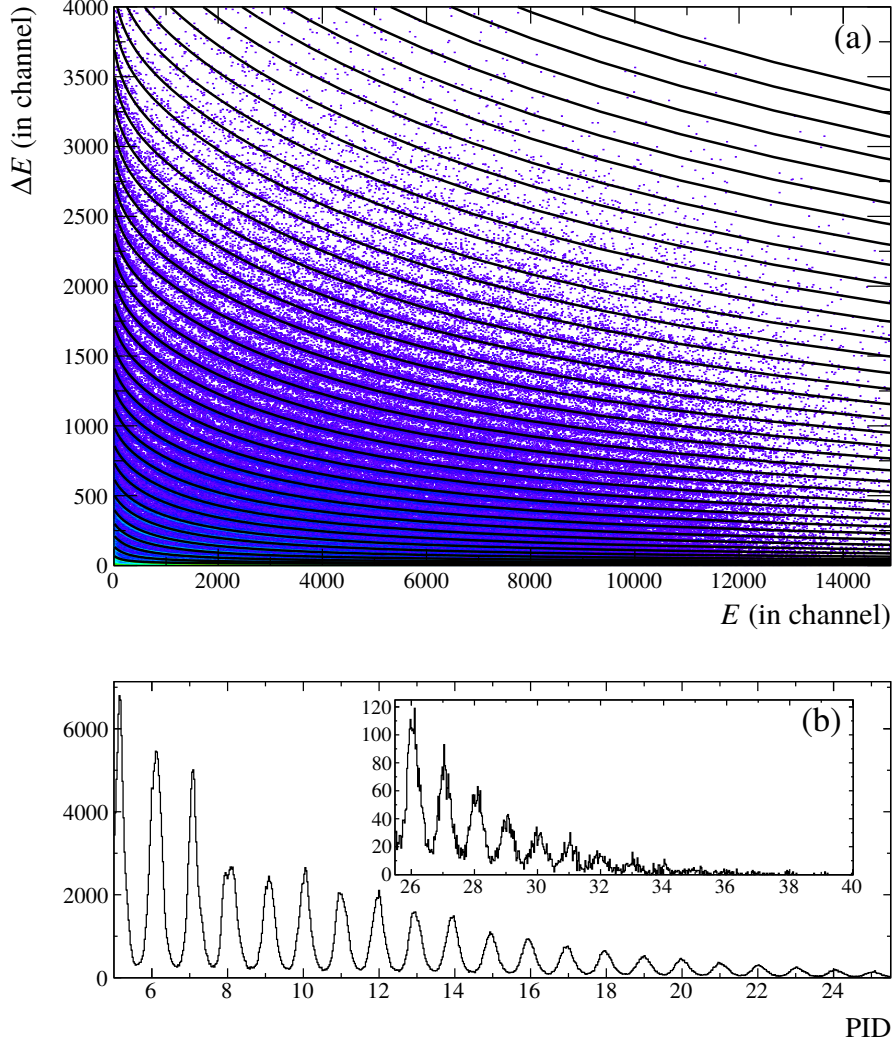


Fig. 6. Example of coupling between the SPIDER identification method and a functional fit [16]. The identification grid used as input is shown in Fig.2.

166 Raw  $Z$ -lines obtained with the SPIDER method on an INDRA Si-CsI(Tl)  
 167 matrix are those previously presented in Fig. 2. These lines, which do not  
 168 cover the whole residual energy range, are used to fit the 9 parameters of the  
 169 functional [16]. The result of the fit is shown in Fig. 6. It can be seen that a  
 170 satisfactory agreement is obtained for all charges and over the full matrix. The  
 171 quality of the charge identification can be checked in Fig. 6: a good charge  
 172 identification is achieved up to  $Z \sim 36$ , even if the statistics for high  $Z$  is very  
 173 poor. The coupling between the SPIDER method and a functional fit allows  
 174 to obtain a full charge identification in a very short time. This procedure was  
 175 used during the data reduction of the INDRA experiment presented in [33].

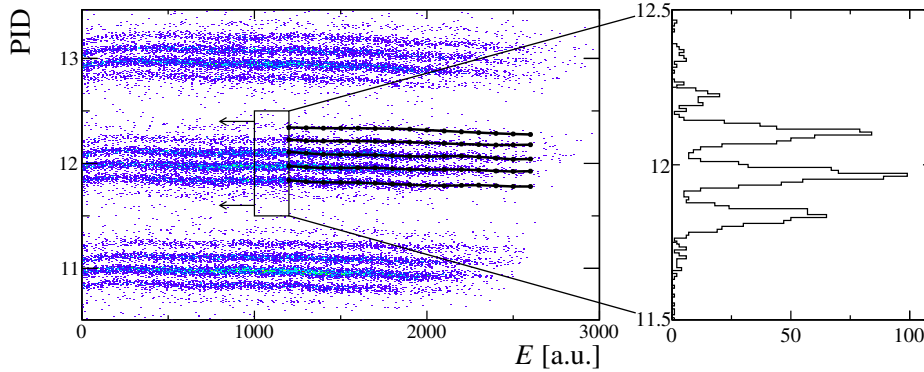


Fig. 7. Illustration of the isotopic identification method in PID- $E$  matrices.

### 176 3 Isotopic identification

177 The method presented above, and its possible coupling with a fitting pro-  
 178 cedure, facilitate a lot the extraction of  $Z$ -identification lines. As illustrated  
 179 in Fig. 4(b), the good quality of FAZIA silicon detectors allows also isotopic  
 180 identification of charged particles up to  $Z \sim 25$ . In order to carry out an  
 181 isotopic identification, ridge lines corresponding to each  $(Z, A)$  couple have  
 182 to be drawn. This is again a very fastidious task. We propose here a method  
 183 to extract these lines in a fully automatic way. The only input of the algo-  
 184 rithm is a charge-identification grid that can be easily generated using the  
 185 SPIDER identification method, which is particularly efficient for the case of  
 186 Si-Si matrices (see Fig. 4).

187 In  $\Delta E - E$  matrices, lines corresponding to a given atomic number  $Z$  are  
 188 regularly spaced and populated. The scheme for isotopic lines is much more  
 189 complex: the relative population of each isotope depends strongly on the con-  
 190 sidered element, on the studied reaction, and isotopes with short lifetimes (typ-  
 191 ically lower than 1 ns) are never detected. The extraction of isotopic  $(Z, A)$ -  
 192 lines from the raw  $\Delta E - E$  matrix is therefore very complex. To simplify the  
 193 treatment, we have to transform the matrix in order to extract masses  $Z$  by  
 194  $Z$ . The first stage of the algorithm is then to linearize the  $\Delta E - E$  matrix  
 195 according to the  $Z$ -identification grid provided by the user, in order to obtain  
 196 a PID- $E$  matrix (Fig. 7). If the quality of the grid is good enough,  $A$ -lines  
 197 associated to a given  $Z$  are almost horizontal and lie in the PID range  $[Z-0.5,$   
 198  $Z+0.5]$ .

199 All points contained in the range  $\text{PID} = Z \pm 0.5$  and  $E = E_i \pm \delta E$  (rectangu-  
 200 lar box in Fig. 7) are projected on the PID axis. Peaks corresponding to the  
 201 intersection of  $A$ -lines and the vertical line  $E = E_i$  appear in the projection  
 202 histogram. The binning of this projection is set to 60 bins whatever the  $Z$   
 203 considered. Peaks are located and replaced in the PID- $E$  matrix. Each new  
 204 point is simply associated to the closest  $A$ -line. The operation is then repeated

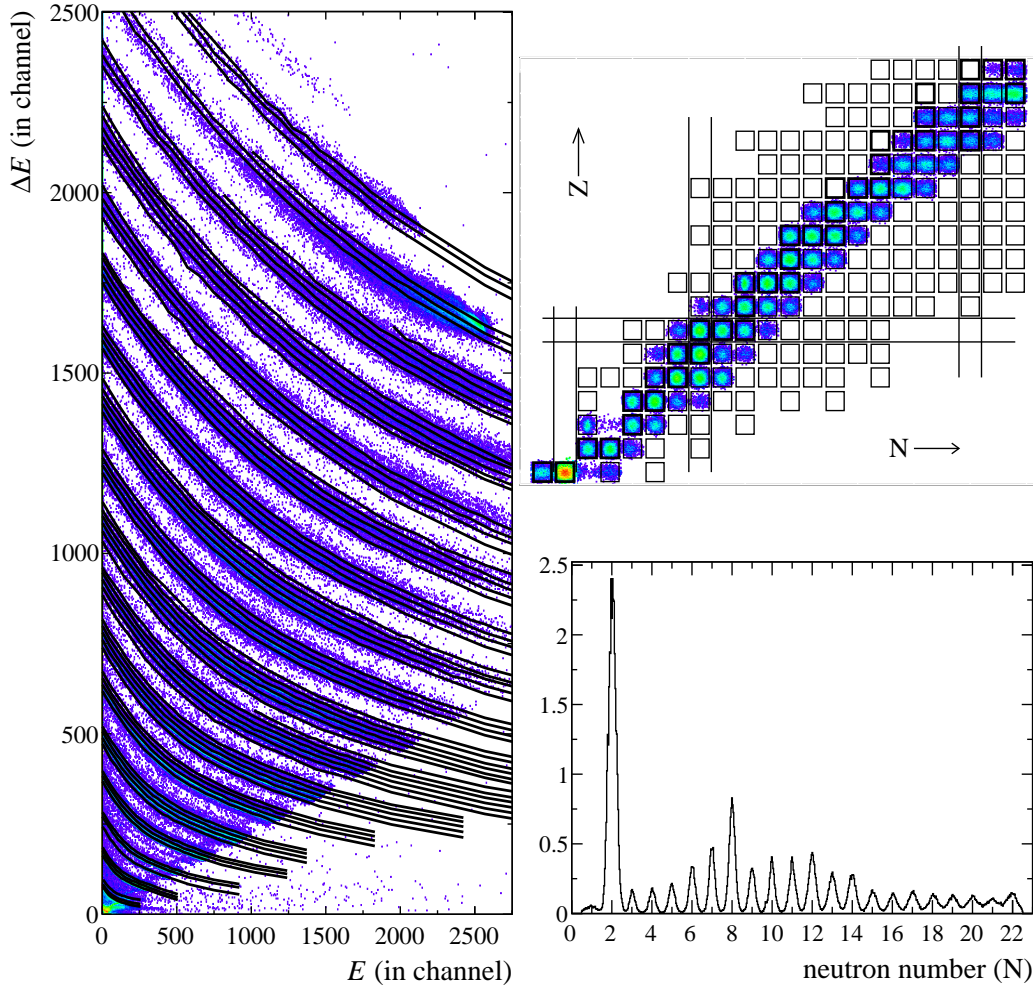


Fig. 8. Result of the automatic isotopic line extraction applied to a Si-Si matrix of FAZIA ( $\theta \sim 7^\circ$ ) in the Ar+Sn at 25 MeV/A reaction: isotopic identification grid, isotopic and neutron number distribution after linearization.

205 by varying  $E_i$  in order to cover the whole residual energy range, and for all  $Z$   
 206 (Fig. 7). The obtained identification grid in the PID- $E$  plane is finally trans-  
 207 formed in the  $\Delta E - E$  plane (Fig. 8). The corresponding isotopic identifica-  
 208 tion matrix is presented in Fig. 8.

209 This algorithm has also been implemented in the identification grid editor of  
 210 KaliVeda [29].

## 211 4 Conclusion

212 In this article, we proposed a new method (SPIDER identification) for gener-  
 213 ating  $Z$  and  $A$  identification grids in two-dimensional matrices. This method

214 has been developed avoiding as much as possible the use of *a priori* infor-  
215 mation on the exact form of identification lines, in order to be applicable to  
216 a large variety of identification matrices. It has been successfully tested on  
217 various types of matrices obtained with  $\Delta E - E$  and Pulse Shape Analysis  
218 techniques. Particular attention has been paid to the implementation in a suit-  
219 able graphical environment, so it needs only two mouse-clicks from the user  
220 in order to calculate all initialization parameters. Extracted lines can then be  
221 directly used to identify charged particles, set as an input of a functional fit,  
222 or used to extract isotopic lines in a fully automatic way.

## 223 5 Acknowledgements

224 The authors express their acknowledgement to the GANIL and LNS accel-  
225 erator staff for their continued support during the experiments. We would  
226 especially like to thank the INDRA and FAZIA collaborations for allowing  
227 us to use their unpublished data. One of us (J.D.F.) would like to thank L.  
228 Tassan-Got for many fruitful discussions and for providing his code which  
229 is used in KaliVeda both for linearization of the identification grids and for  
230 fitting to his identification functional(s). This work was supported by the Pol-  
231 ish National Science Centre under Contract No. UMO-2014/14/M/ST2/00738  
232 (COPIN-INFN Collaboration) and Contract No. UMO-2013/08/M/ST2/0025  
233 (LEA-COPIGAL).

## 234 References

- 235 [1] Ph. Chomaz, F. Gulminelli, W. Trautmann, S. J. Yennello, Eur. Phys. J. A 30  
236 (2006).
- 237 [2] B. Borderie and M. F. Rivet, Prog. Part. Nucl. Phys. 61 (2008) 551.
- 238 [3] D.W. Stracener et al., Nucl. Instr. Meth. Phys. Res. A 294 (1990) 485.
- 239 [4] J. Pouthas et al., Nucl. Instr. Meth. Phys. Res. A 357 (1995) 418.
- 240 [5] K Kwiatkowski et al., Nucl. Instr. Meth. Phys. Res. A 360 (1995) 571.
- 241 [6] D.G. Sarantites et al., Nucl. Instr. Meth. Phys. Res. A 381 (1996) 418.
- 242 [7] A. Pagano et al., Nuclear Physics A 734 (2004) 504.
- 243 [8] S. Wuenschel et al., Nucl. Instr. Meth. Phys. Res. A 604 (2009) 578.
- 244 [9] R. Bougault et al., Eur. Phys. J. A 50 (2014) 47.
- 245 [10] J. Lukasik et al., Nucl. Instr. Meth. Phys. Res. A 709 (2013) 120.

- 246 [11] S. Barlini et al., Nucl. Instr. Meth. Phys. Res. A 600 (2009) 644.
- 247 [12] L. Bardelli et al., Nucl. Instr. Meth. Phys. Res. A 654 (2011) 272.
- 248 [13] J.L. Flores et al., Nucl. Instr. Meth. Phys. Res. A 830 (2016) 287.
- 249 [14] F. S. Goulding, D. A. Landis, J. Cerny, R. H. Pehl, Nucl. Instr. Meth. 31 (1963)  
250 1.
- 251 [15] G. W. Butler, A. M. Poskanzer, and D. A. Landis, Nucl. Instr. Meth. 89 (1970)  
252 189.
- 253 [16] L. Tassan-Got, Nucl. Instr. Meth. Phys. Res. B 194 (2002) 503.
- 254 [17] N. Le Neindre et al., Nucl. Instr. Meth. Phys. Res. A 490 (2002) 251.
- 255 [18] M. Pârlog et al., Nucl. Instr. Meth. Phys. Res. A 482 (2002) 674.
- 256 [19] G. Tabacaru et al., Nucl. Instr. Meth. Phys. Res. A 428 (1999) 379.
- 257 [20] P.F. Mastinu et al., Nucl. Instr. Meth. Phys. Res. A 371 (1996) 510.
- 258 [21] T. Cap et al., Phys. Scr. T154 (2013) 014007.
- 259 [22] A. Benkirane et al., Nucl. Instr. Meth. Phys. Res. A 355 (1995) 559.
- 260 [23] C.M. Iacono Manno et al., Nucl. Instr. Meth. Phys. Res. A 443 (2000) 503.
- 261 [24] R. Wirth et al., Nucl. Instr. Meth. Phys. Res. A 717 (2013) 77.
- 262 [25] M. Morháč and M. Veselský, Nucl. Instr. Meth. Phys. Res. A 592 (2008) 434.
- 263 [26] L. Morelli et al., Nucl. Instr. Meth. Phys. Res. A 620 (2010) 305.
- 264 [27] J. Dudouet et al., Nucl. Instr. Meth. Phys. Res. A 715 (2013) 98.
- 265 [28] R. Brun, Nucl. Instr. Meth. Phys. Res. A 389 (1997) 81.
- 266 [29] J.D. Frankland, et al., <http://indra.in2p3.fr/KaliVedaDoc>.
- 267 [30] M. Morháč et al., Nucl. Instr. Meth. Phys. Res. A 443 (200) 108.
- 268 [31] S. Barlini et al., Physical review C 87 (2013) 054607.
- 269 [32] S. Piantelli et al., Physical review C 88 (2013)064607 .
- 270 [33] J.D. Frankland, D. Gruyer, E. Bonnet, and A. Chbihi, EPJ Web of Conferences  
271 88 (2015) 00009.